

An averaged polarizable potential for multiscale modeling in phospholipid membranes

Witzke, Sarah; List, Nanna Holmgaard; Olsen, Jógvan Magnus Haugaard; Svendsen, Casper Steinmann; Petersen, Michael; Beerepoot, Maarten T. P.; Kongsted, Jacob

Published in:
Journal of Computational Chemistry

DOI (link to publication from Publisher):
[10.1002/jcc.24718](https://doi.org/10.1002/jcc.24718)

Creative Commons License
CC BY-NC 4.0

Publication date:
2017

Document Version
Early version, also known as pre-print

[Link to publication from Aalborg University](#)

Citation for published version (APA):
Witzke, S., List, N. H., Olsen, J. M. H., Svendsen, C. S., Petersen, M., Beerepoot, M. T. P., & Kongsted, J. (2017). An averaged polarizable potential for multiscale modeling in phospholipid membranes. *Journal of Computational Chemistry*, 38(9), 601-611. <https://doi.org/10.1002/jcc.24718>

General rights

Copyright and moral rights for the publications made accessible in the public portal are retained by the authors and/or other copyright owners and it is a condition of accessing publications that users recognise and abide by the legal requirements associated with these rights.

- Users may download and print one copy of any publication from the public portal for the purpose of private study or research.
- You may not further distribute the material or use it for any profit-making activity or commercial gain
- You may freely distribute the URL identifying the publication in the public portal -

Take down policy

If you believe that this document breaches copyright please contact us at vbn@aub.aau.dk providing details, and we will remove access to the work immediately and investigate your claim.

An Averaged Polarizable Potential for Multiscale Modeling in Phospholipid Membranes

Sarah Witzke*, Nanna Holmgaard List†, Jógvan Magnus Haugaard Olsen*,
Casper Steinmann‡, Michael Petersen*, Maarten T. P. Beerepoot§, Jacob Kongsted*

kongsted@sdu.dk

Abstract

A set of average atom-centered charges and polarizabilities has been developed for three types of phospholipids for use in polarizable embedding calculations. The lipids investigated are 1,2-dimyristoyl-*sn*-glycero-3-phosphocholine (DMPC), 1-palmitoyl-2-oleoyl-*sn*-glycero-3-phosphocholine (POPC) and 1-palmitoyl-2-oleoyl-*sn*-glycerol-3-phospho-L-serine (POPS) given their common use both in experimental and computational studies. The charges, and to a lesser extent the polarizabilities, are found to depend strongly on the molecular conformation of the lipids. Furthermore, the importance of explicit polarization is underlined for the description of larger assemblies of lipids, *i.e.* membranes. In conclusion, we find that specially developed polarizable parameters are needed for embedding calculations in membranes, while common non-polarizable point-charge force fields usually perform well enough for structural and dynamical studies.

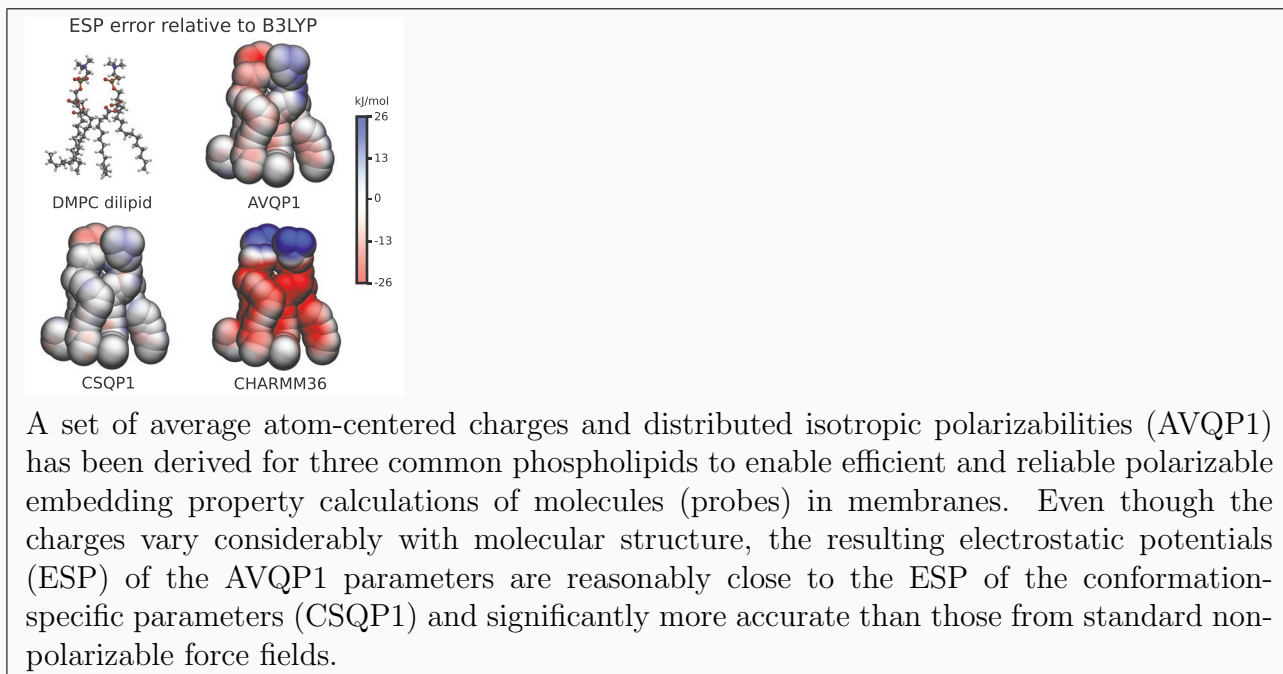
Keywords: Multiscale modeling, Polarizable Embedding, QM/MM, Lipid Membrane, Prodan. ■

*Department of Physics, Chemistry and Pharmacy, University of Southern Denmark, DK-5230 Odense M, Denmark

†Division of Theoretical Chemistry and Biology, School of Biotechnology, KTH Royal Institute of Technology, SE-106 91 Stockholm, Sweden

‡Centre for Computational Chemistry, School of Chemistry, University of Bristol, Bristol BS8 1TS, United Kingdom

§Centre for Theoretical and Computational Chemistry, Department of Chemistry, University of Tromsø—The Arctic University of Norway, N-9037 Tromsø, Norway



INTRODUCTION

During the last couple of decades computer simulations have become an increasingly important tool in the investigation of biological systems. Simulations offer insight on a detailed and atomistic level not easily probed by experimental techniques. An example of this is the electronic transitions occurring upon excitation of a probe in a lipid membrane. Investigation of such systems can be described using hybrid models where the probe—and perhaps the closest lipid molecules—are treated at the quantum mechanical (QM) level while the remainder of the system is treated classically with molecular mechanics (MM), *i.e.* a QM/MM model.¹⁻³ The energy functions, or force fields, used in standard MM models usually do not include polarization explicitly, leading to several shortcomings in for example a QM/MM study of a probe in a lipid bilayer. Firstly, somewhere between 6 and 30% of the total electrostatic interaction energy is due to polarization,⁴⁻⁹ meaning that a large portion of the electrostatic energy is discarded when polarization is excluded. An implicit account of polarization might be achieved using enhanced values for the point charges, but this is not a rigorous treatment of the effect. Secondly, changes in the charge distribution of a QM region cannot propagate

to the surrounding MM environment with fixed-charge force fields, underlining their limitations. Thirdly, lipid bilayers are highly heterogeneous systems consisting of both a non-polar core of hydrocarbon tails and an interface region of charged and polar groups interacting with an aqueous solvent. Both the interface and the core are in fact inadequately described by fixed-charge force fields: It has been shown that non-polarizable force fields inaccurately predict the dielectric constant for alkanes¹⁰ and that this affects, for instance, ion channel proteins in lipid bilayers.^{11,12} In their review of explicit inclusion of electronic polarization in MM simulations, Lopes *et al.*¹³ account for several systems where polarization is important including ions and highly polar groups in water as well as heterogeneous non-polar environments, *i.e.* exactly what indicates a lipid membrane. As such, several studies have recognized the importance of expanding standard MM force fields to include polarization effects. A popular approach to include polarization is the induced-dipole model¹⁴ as implemented in for instance AMOEBA,^{15,16} Amber02¹⁷ and PFF.¹⁸ Basically, in this approach each atom is described by a polarizability, in addition to a charge, giving rise to an induced dipole moment, thereby greatly increasing the flexibility compared to standard fixed-charge force fields. Another widely used model for including polarization in simulations is through the classical Drude model,^{19,20} where a given atom in the system is replaced by a central particle carrying all (or the majority of the) mass and a so-called Drude particle connected to the central atom via a spring. Both particles are charged, hence in effect describing a dipole able to vary in magnitude and direction in response to the environment. Within the last couple of years several polarizable lipid models have been developed based on the classical Drude model.^{21–24}

Another aspect of standard force fields is that they treat electrostatic interactions with a Coulombic potential between atom pairs, where each atom is assigned a fixed charge. This means that the charges modeling the true charge distribution cannot adapt to changes in the molecular conformations or in the local electric fields. Conformational aspects may to some extent be implicitly included by deriving charges from different molecular conformations and then invoking an averaging procedure as done for instance in the Amber set of force fields.^{25,26} The charges in standard force fields are normally obtained by a fitting procedure where the aim is to reproduce the molecular electrostatic potential (ESP) from a QM

reference calculation. For this, several different schemes are available, e.g. RESP,²⁷ MK,²⁸ HLY²⁹ and CHelpG.³⁰ It is well known that ESP-fitted charges depend strongly on the given conformation of the molecule,^{31–35} and different attempts have been made to alleviate this problem, for instance by fixing some charges.³⁶ However, there will always remain a certain lack of transferability of charges both between different conformations and between different molecules. A way to alleviate this is to include polarizabilities in the force field. Even though polarizabilities are also sensitive to the molecular conformation as discussed by Söderhjelm *et al.*,³⁷ the conformational dependence is less than that for ESP-fitted charges. This suggests that a combination of ESP-fitted charges and isotropic polarizabilities could to some extent make up for the loss of accuracy when using average charges.

In this paper our primary aim is to develop the electrostatic component of a polarizable force field with prospective use in polarizable embedding (PE) calculations,^{38,39} *i.e.* an embedding potential. Use of polarizable force fields is especially important in situations where the molecule under study is exposed to a varying electric field or if the charge distribution of the molecule is strongly coupled to its environment. This is why we apply the parameters to the optical properties of a membrane probe, where excitation leads to a redistribution of the electron density in the probe. Explicit polarization is expected to be important to adequately allow the probe and environment to adjust to this event.

We further investigate to what extent a fixed-charge approximation is valid for the range of lipid conformations found in a membrane. This is done by calculating a large set of ESP-fitted charges and investigating the fluctuation of the charges, thereby directly quantifying the conformational dependence. Three common lipid types are studied, namely 1,2-dimyristoyl-*sn*-glycero-3-phosphocholine (DMPC), 1-palmitoyl-2-oleoyl-*sn*-glycero-3-phosphocholine (POPC) and 1-palmitoyl-2-oleoyl-*sn*-glycerol-3-phospho-L-serine (POPS). Chemical structures of the head and tail groups are shown in Figure S1 in the supporting information. Based on the charges from different lipid conformations, a set of averaged charges is derived. The conformational dependence of the isotropic polarizabilities is also examined and averaged parameters are similarly derived. For the calculations of charges and polarizabilities we rely on a fragmentation procedure and derive all quantities from *ab-initio* calculations.

The paper is organized as follows: the methodology section describes how the averaged

parameters are obtained and how their accuracy is tested. In the results and discussion, we start by identifying a good fragmentation approach to obtain the atom-centered charges and polarizabilities, and discuss intra- and intermolecular polarization effects. Second, we discuss the conformational dependence of the parameters and test the quality of a fixed-charge approximation. Third, the averaged parameters are used in an example calculation to determine optical properties of the membrane probe Prodan. Finally, we sum up the main conclusions in this paper.

METHODOLOGY

The generation and testing of the embedding parameters, in this work referred to as ‘QP1’ where Q denotes ESP-fitted charges and P1 denotes isotropic polarizabilities, involves a number of steps. The first step is the fragmentation of the lipid. Electronic structure calculations were performed on three representative lipid conformations that had been fragmented in different ways and their ESPs are compared to ESPs for the corresponding unfragmented lipids. The second step is the calculation of atom-centered charges and isotropic polarizabilities for a large number of lipid molecules from a simulation of a lipid bilayer using the chosen fragmentation scheme. The third step is the investigation of conformational dependencies and determination of a set of average parameters. The parameters are here averaged over 200 lipid conformations of each lipid type. This strategy of extracting molecular conformations from a simulation and averaging the electrostatic parameters is similar to the approach used in the Slipid,^{40–42} GAFFlipid,⁴³ Lipid11,⁴⁴ and Lipid14⁴⁵ force fields. Different methods to calculate the parameters are compared by calculating the root-mean-square deviation (RMSD) of the ESP for the parameters and for a QM reference. Embedding potentials based on the average parameters are compared to other force fields in an application to the optical properties of Prodan, a membrane probe, embedded in a lipid bilayer. Details on the generation of the lipid conformations, fragmentation procedure, the calculation of embedding parameters, the evaluation of the electrostatic potentials and the calculation of the optical properties of Prodan are detailed below.

Generation of Lipid Conformations

To sample different lipid conformations, MD simulations of hydrated membranes of either DMPC, POPC or POPS lipids were run in the *NPT* ensemble in the Amber 12⁴⁶ MD package for more than 100 ns at 310 K. The three lipid types were described by the CHARMM36 force field⁴⁷ and water by the TIP3P model.⁴⁸ One snapshot was extracted for each system at the end of the simulation. Further details regarding the initial structures, and equilibration and simulation protocol are provided in the supporting information, where also figures of each lipid type with the CHARMM36 atom names are included (Figure S1).

Average atom-centered charges and polarizabilities for POPC lipid molecules were calculated for both a bilayer hydrated in 150 mM NaCl solution and in pure water. The differences in both charges and polarizabilities between the POPC lipids in each system were so small that we conclude that an addition of 150 mM NaCl does not change the ensemble conformation of the lipids to a degree that impacts the final averaged charges and polarizabilities. Therefore, all results in the following are based on simulations of lipid bilayers hydrated in a 150 mM NaCl solution.

Fragmentation Procedure

To reduce the computational cost of generating embedding potentials, each lipid molecule is fragmented into smaller constituents. When performing an electronic structure calculation, polarization between the atoms in a given molecule is already included. Thus, atoms within a given molecule or molecular fragment should not polarize each other in subsequent calculations since polarization effects would in that case be included twice. Each lipid molecule is cut into smaller fragments on which electronic structure calculations are performed to obtain atom-centered charges and polarizabilities. The atoms within each fragment are still not allowed to polarize each other, but polarization between the fragments is allowed. In this way one part of a lipid molecule can interact with another part of the same lipid provided the atoms are in different fragments, and thus potentially reduce the error that is introduced by the fragmentation. To avoid polarization between atomic sites within the same frag-

ment, exclusion lists are created with atom pairs for which polarization should be excluded. Exclusion lists for each of the three lipids are included as supporting information.

The size of the fragments and hence the number of fragments in each lipid molecule is a compromise between computational cost and accuracy. A chemically sound fragmentation pattern is to cut each lipid molecule into three fragments: two tail fragments and one head-group fragment. Caps are added according to the molecular fractionation with conjugate caps (MFCC) model⁴⁹ to all radical groups to saturate open valencies in a way mimicking the neighboring fragment. Figure 1 exemplifies the MFCC procedure for a DMPC lipid (corresponding to fragmentation pattern F2C3 in Figure 2). The lipid has been decomposed into three fragments, which are capped with part of the neighboring fragment (the capping groups are shown in red and blue). The cap is properly terminated with hydrogen atoms, positioned along the original bond but with a bond vector scaled to a length of 0.96 Å for O-H bonds and 1.09 Å for C-H bonds. In addition, the caps of neighboring fragments are combined to form so-called concaps, whose contributions are subtracted to avoid double counting and to compensate for the error due to the caps. The MFCC model was applied to localized properties following Söderhjelm and Ryde⁹ and the fragmentation and capping process was performed using FragIt.⁵⁰

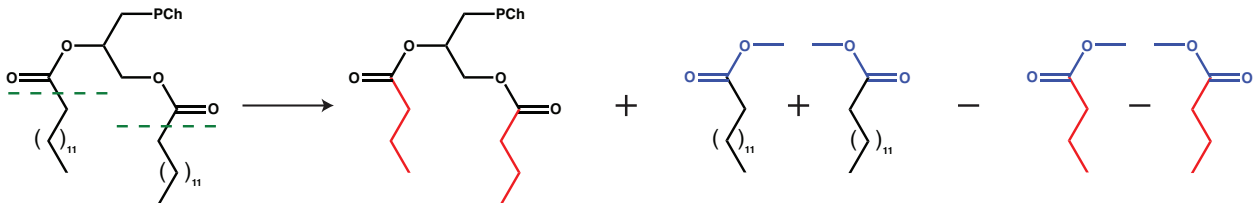


Figure 1: The MFCC procedure for fragmentation pattern F2C3 of DMPC. PCh: Phosphocholine. The lipid molecule is fragmented at the position of the *green*, dashed lines, the added caps are indicated in *red* and *blue*. See Figure 2 for the fragmentation nomenclature.

Six different fragmentation patterns are considered. Each fragmentation pattern is defined using an FxCy notation, where x denotes the fragmentation site and y the size of the capping group. A schematic representation of the different fragmentation patterns is shown in Figure 2. Three different fragmentation sites, $x=1-3$, and cap sizes, $y=1-3$, have been investigated. Only two cap sizes per fragmentation site have been considered due to current

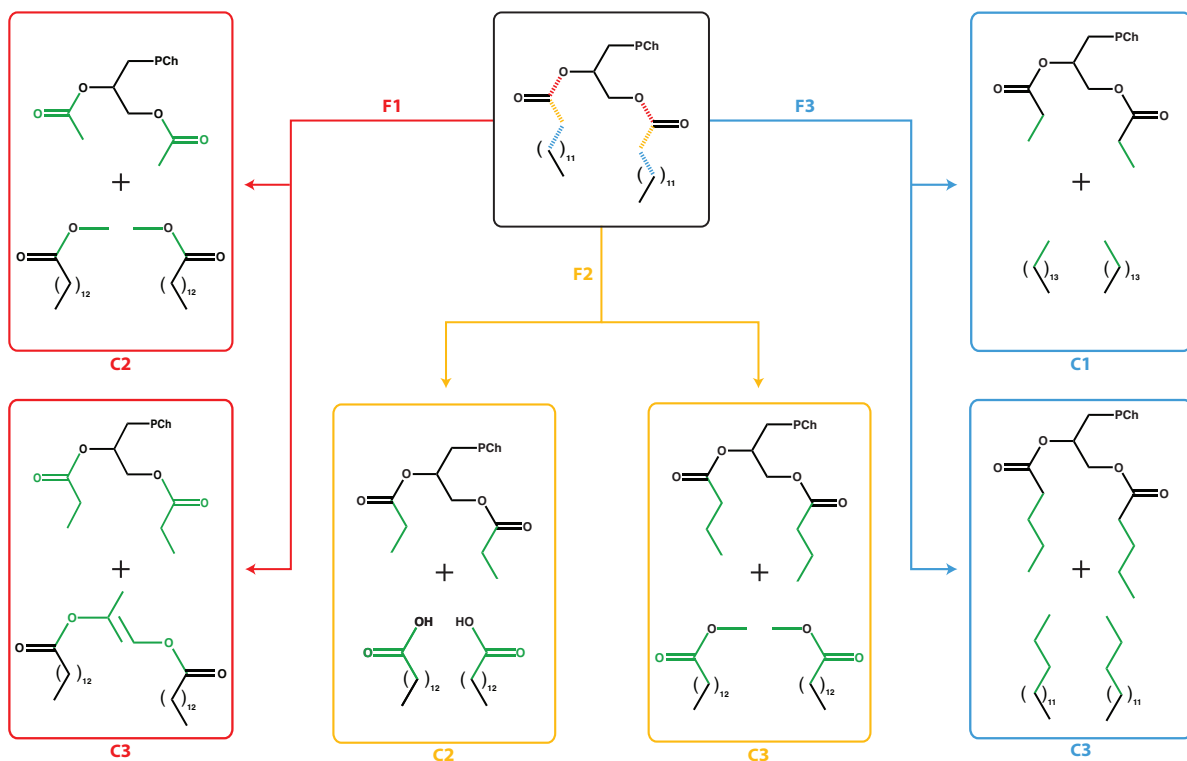


Figure 2: The six fragmentation patterns tested for DMPC. The three fragmentation sites, F1, F2 and F3, are shown in red, yellow and blue, respectively. Caps are shown in green, and the cap size, C1, C2 or C3, is stated for each branch.

limitations in FragIt. The different fragmentation patterns are only tested on three conformations of DMPC under the assumption that the differences in fragmentation patterns found for DMPC are directly transferable to POPC and POPS.

Embedding Potential Parameters

The restrained electrostatic potential (RESP) method²⁷ was used for the generation of ESP-fitted charges. The ESP used in the fitting was generated by Gaussian 09,⁵¹ while the fitting was performed using the Antechamber^{52,53} module from the AmberTools12 package.⁴⁶ The grid points were sampled by the Merz–Kollman (MK) scheme²⁸ on ten molecular surfaces between 1.4 and 2.7 times the van der Waals radius of the lipid atoms using a grid point density of 17 \AA^{-2} , *i.e.*, a higher point density as recommended by Sigfridsson and Ryde.⁵⁴ The

distributed (atom-centered) polarizabilities were evaluated within the localized properties (LoProp) scheme⁵⁵ implemented in the MOLCAS 7 program.^{56,57} Following our previous study on protein embedding potentials,⁵⁸ the aug-cc-pVDZ⁵⁹⁻⁶¹ basis set was used for the average embedding potentials. Even though (close to) basis set convergence of especially the isotropic polarizabilities is reached only at the aug-cc-pVTZ level,^{37,62} the error in the ESP introduced by using the aug-cc-pVDZ basis set has been found to be small.⁶² The B3LYP functional⁶³⁻⁶⁷ was used both in the preliminary analysis and to calculate the average parameters.

An initial analysis showed that charges fitted with either the MK,²⁸ CHelpG³⁰ or HLY²⁹ procedures all performed slightly better than RESP charges in reproducing the QM ESP of a given conformation of a lipid molecule. When using average (here referred to as ‘AV’) charges, however, the RESP charge model yields ESPs closer to the full QM ESP than the MK fitting model. This indicates that constraining the charges of chemically equivalent atoms can best be done within the ESP fitting, rather than after it. These results are in agreement with the work of Beerepoot *et al.*: the error made in the averaging of ESP-fitted charges is much lower for RESP than for other ESP-fitting schemes, which more than compensates for the less accurate conformation-specific (CS) ESP.⁶² Another feature of the RESP procedure is that the charges are restrained towards zero, which reduces the conformational dependence on especially the buried charges.²⁷ The latter restraint, however, is not a necessity when the averaging over different conformations is explicitly accounted for as in this work. We thus use RESP charges for the average parameters in this work, but advice the use of other ESP-fitting schemes for work in which the charges are generated for every geometry separately.

Isotropic polarizabilities are used rather than anisotropic ones in order to ensure transferability of parameters between different molecular conformations. Previous studies have shown that isotropic polarizabilities perform almost as well as their anisotropic counterparts even though the impact of anisotropy becomes increasingly important at short distances and for molecules that are highly polarizable.^{38,58,68} Neither of these cases are of great relevance for lipid membranes.

Electrostatic Potential Analysis

Classical ESPs were compared to a reference QM ESP on the unfragmented lipid. Classical ESPs were calculated for the parameters developed in this work as well as for several charge sets from the literature, namely i) the united-atom lipid charges from Chiu *et al.*,⁶⁹ which are used in the Gromos^{70–72} and Berger⁷³ force fields; ii) General Amber Force Field for Lipids (GAFFlipid)⁴³ from the Lipidbook repository⁷⁴; iii) Lipid14,⁴⁵ which was complemented with the parameters from Lipid11⁴⁴ for POPS, both obtained through the Amber14⁷⁵ package iv) Slipid^{40–42} from the Lipidbook repository⁷⁴ and v) CHARMM36⁴⁷ obtained together with the membrane coordinates obtained from the CHARMM-GUI Membrane Builder.⁷⁶ The latter four are all-atom force fields and GAFFlipid, Lipid14 and Slipid are all based on RESP charges averaged over different conformations. The classical ESPs were obtained using the PE library,⁷⁷ while the QM ESPs were calculated using the LSDalton program.^{78,79} The reference QM ESP was calculated with the same QM method (B3LYP^{63–67}/aug-cc-pVDZ^{59–61}) as the embedding potential parameters. We note, however, that self-interaction errors can affect B3LYP results on a large anionic molecule such as the POPS lipid.^{80,81}

All ESPs were calculated on a cubic grid of uniformly distributed points with a density of 4 points per bohr. The classical and QM ESPs were compared by calculating RMSDs based on points on a molecular surface defined by twice the van der Waals (vdW) atomic radii. All points within factors 2.00 ± 0.01 from this surface were included in the RMSD value, *i.e.*, we use only points within the range where the fitting was performed. The distance of 2 Å corresponds approximately to the intermolecular distances that are relevant for our purposes and was chosen based on work performed by Olsen *et al.*⁵⁸ We note that the same procedure was used to test the solvent embedding parameters in ref. 62, where it was also shown that relative differences between different ESPs are rather independent of the distance from the molecule at which the ESPs were evaluated.⁶² For further details regarding the generation of ESPs we refer to ref. 58. All RMSDs are provided as energies from the interaction with an elementary point charge.

Optical Properties of Prodan

The lowest excitation energy and associated oscillator strength were calculated for Prodan in vacuum and for a snapshot of Prodan embedded in a lipid bilayer of either POPC or DMPC. The simulation details are described in the Supporting Information.

The geometry of Prodan was optimized at the B3LYP/6-311++G**⁸²⁻⁸⁵ level of theory in a dielectric continuum with a static dielectric constant ($\epsilon=4$), simulating the interior of a lipid bilayer. The IEF-PCM^{86,87} polarizable continuum model in Gaussian 09⁵¹ was used to model the effects of the bilayer in the geometry optimization, adopting cavity radii defined according to Gaussian 09 defaults. The geometry-optimized structure of Prodan was also used to calculate the optical properties of Prodan embedded in the lipid bilayers so that all differences are due to the description of the environment only. The excitation energy and oscillator strength of the lowest excited state were computed using the PE-TD-DFT³⁸ model using either average parameters from this study (charges with and without polarizabilities) or charges from standard lipid force fields. The calculations were performed in Dalton 2013,^{78,88} using the PE library⁷⁷ and Gen1Int for the one-electron integrals^{89,90} with the CAM-B3LYP functional⁹¹ together with the 6-31+G*^{84,92-94} basis set.

RESULTS AND DISCUSSION

In this section we first investigate different fragmentation schemes and discuss intra- and intermolecular polarization effects. Second, we discuss the conformational dependence of charges and polarizabilities calculated for each individual lipid in model membranes consisting of 200 lipids. Finally, these average parameters are used in a preliminary application of the membrane-embedded probe Prodan. In the following all charges and polarizabilities are given in atomic units (a.u.).

Fragmentation Procedure

The analysis of the different fragmentation procedures is done on three different conformations of a DMPC lipid extracted from the MD simulation. Three lipids with different

geometries were chosen as representative examples in order to sample different lipid conformations.

The RMSD values of the ESP error for the studied fragmentation patterns are compiled in Table 1. Included are RMSDs for ESPs produced from RESP charges (denoted Q) as well as for ESPs produced from RESP charges and LoProp isotropic polarizabilities (denoted QP1). Additional data for LoProp multipoles and anisotropic polarizabilities are shown in Table S3 in the supporting information. The performance of all the fragmentation patterns depends on the specific conformation of the lipid (**1**, **2** or **3**). Overall, fragmentation pattern F2C3 performs best for the isotropic parameters (Table 1) as well as for the anisotropic LoProp parameters (Table S3 in the supporting information), and we thus continue using the F2C3 fragmentation pattern.

Table 1: RMSD values [kJ mol^{-1}] for the ESP from classical parameters (calculated with different fragmentation procedures) with respect to a full QM reference ESP on three conformations of DMPC (**1**, **2** and **3**). Classical conformation-specific parameters and the QM reference were calculated with B3LYP/aug-cc-pVDZ. The classical ESPs are based on RESP charges (denoted Q), or RESP charges and LoProp isotropic polarizabilities (denoted QP1). The right column gives averaged RMSD values over the three conformations.

	DMPC 1		DMPC 2		DMPC 3		Average	
	Q	QP1	Q	QP1	Q	QP1	Q	QP1
F1C2	3.82	4.18	3.86	4.16	4.33	4.28	4.00	4.11
F1C3	3.91	4.30	4.00	4.76	4.36	4.60	4.09	4.55
F2C2	4.03	4.81	3.83	3.97	4.39	4.65	4.08	4.48
F2C3	3.73	3.83	3.65	3.74	4.36	4.47	3.91	4.01
F3C1	4.43	4.26	4.15	3.99	4.66	4.48	4.41	4.24
F3C3	3.86	3.94	3.92	4.02	4.32	4.53	4.03	4.16

From the RMSD values in Table 1 it is observed that, in most cases, including polarizabilities yields a poorer fit to the full QM ESP. The reason for this is most likely that small inaccuracies around the fragmentation sites are enlarged due to the iterative nature of the

determination of the induced dipole moments. To investigate this behavior further, we considered a 'dilipid' system, obtained as a neighboring pair of lipids from the membrane MD simulation. Because a lipid bilayer consists of many molecules together and since polarization is a many-body effect, a dilipid system will take into account some of these intermolecular interactions. The RMSD between the full QM ESP and a classical ESP produced by only charges was 5.93 kJ mol⁻¹. When isotropic polarizabilities are included, the RMSD value is reduced to 4.28 kJ mol⁻¹. This shows that the inclusion of polarizabilities is beneficial for larger systems with a gain exceeding the error introduced by the fragmentation. This advantage of polarization is illustrated in Figure 3, where c) is the difference of the full QM ESP and a classical ESP from charges (Q) derived in this work, while d) is the difference from the full QM ESP and the classical ESP from charges and polarizabilities (QP1). The error is smallest when both charges and polarizabilities are used.

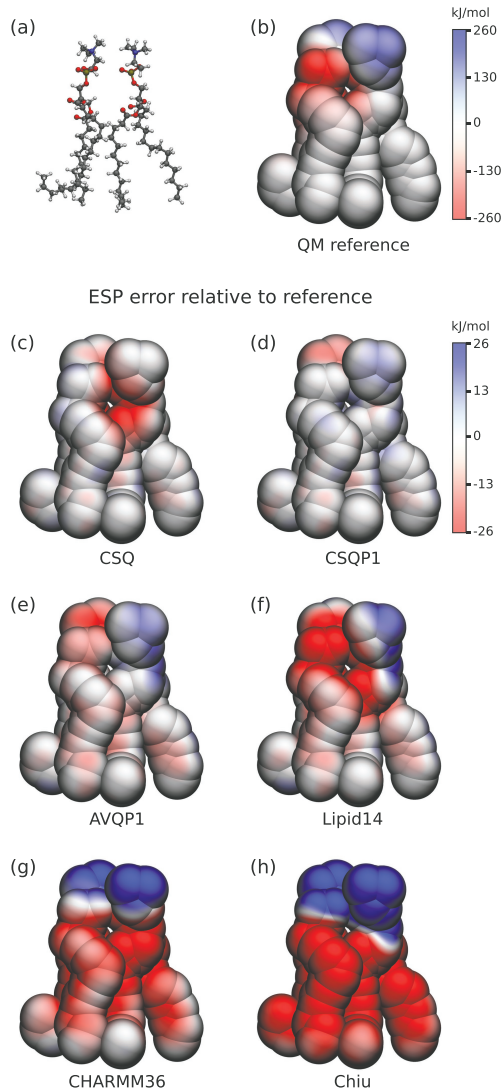


Figure 3: ESP surface plots for the dilipid. a) Ball-and-stick model of the dilipid. b) ESP from a full QM (B3LYP/aug-cc-pVDZ) calculation. Difference between the QM ESP and the ESP generated by the embedding potential based on c) conformation-specific RESP charges (CSQ) d) conformation-specific RESP charges and isotropic polarizabilities (CSQP1), e) average RESP charges and isotropic polarizabilities (AVQP1), f) Lipid14 charges,⁴⁵ g) CHARMM36⁴⁷ charges and h) Chiu⁶⁹ charges. The surfaces are defined by twice the vdW atomic radii. Note the difference in color scale between b) (absolute ESP) and c)-h) (ESP difference).

Included in Figure 3 are also the difference ESPs based on charges from either f) Lipid14⁴⁵, g) CHARMM36⁴⁷ or h) the united-atom force field from Chiu *et al.*⁶⁹, as well as e) the dif-

ference in ESP from the average charges and polarizabilities derived in this work and the total QM ESP shown in b). These other force fields are discussed in subsequent sections.

Analysis of the Average Parameters

A larger set of lipid molecules was studied with the fragmentation scheme F2C3. From each of the four MD membrane simulations (DMPC 150 mM NaCl, POPC in pure water, POPC 150 mM NaCl and POPS 150 mM NaCl), a snapshot was extracted, all 200 lipid molecules fragmented and the atom-centered charges and isotropic polarizabilities calculated at the B3LYP/aug-cc-pVDZ level of theory. The average parameters are printed in Tables S4–S6 in the Supporting Information. The conformational variation of the charges is illustrated in Figure 4 for POPS.

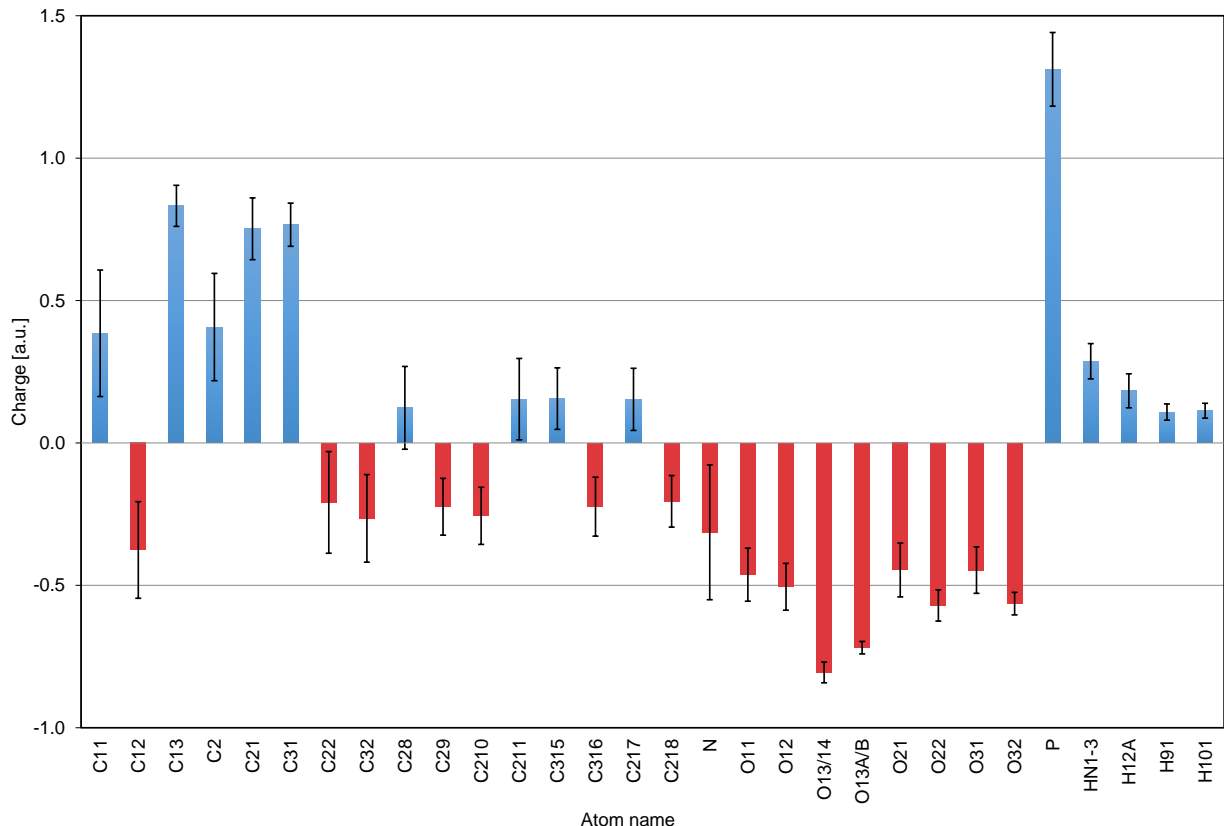


Figure 4: Average (AV) RESP charges for atoms in POPS for average charges greater in magnitude than ± 0.1 . The AV charges for the 200 lipid molecules in the POPS membrane are shown as blue (positive charges) and red (negative charges) bars, and the standard deviations for the averages as black bars.

For all four membrane systems the double bonded oxygens have the most negative charges and show relatively small standard deviations, while the single bonded oxygens are less negative and have a larger standard deviation. The nitrogen atom in POPS has an average charge of -0.31 ± 0.24 , while it has a positive average charge around $+0.19 \pm 0.08$ for both the DMPC and the POPC systems. The difference of the nitrogen charges in the different lipid types is not unexpected, since in POPS the nitrogen is part of a serine moiety while it is part of a choline moiety in DMPC and POPC. All the hydrogens and the majority of the carbon atoms have average charges close to zero. The carbons attached to the choline-nitrogen in DMPC and POPC have negative average charges, together with the first methylene carbons and the terminal methyl carbons in the tails, and the double bonded carbons in POPC

and POPS. The second last carbon atoms in the lipid tails have positive charges, as do the carbonyl carbons of the ester groups, the first carbon after the phosphate group in the head group and the *sn*-2 carbon. The standard deviations for the hydrogens are less than 0.08, while the carbon atoms in general have a larger standard deviation than any of the other elements, agreeing with earlier work on solvent molecules.⁶² Indeed, for the PC (*i.e.* DMPC and POPC) lipids the maximum standard deviation is found for the methylene carbon next to the nitrogen (around 0.20), while for POPS the largest standard deviation is for the nitrogen atom (0.24). For all the four membranes the average charge on phosphorus is +1.3 with a standard deviation around 0.1. Several of the charges show very large conformational dependence, e.g. for POPS the charge of the nitrogen varies between -1.1 and $+0.51$, and the charge of the C11 atom varies between -0.066 and $+1.49$, which questions the validity of a fixed-charge model for the lipid types investigated.

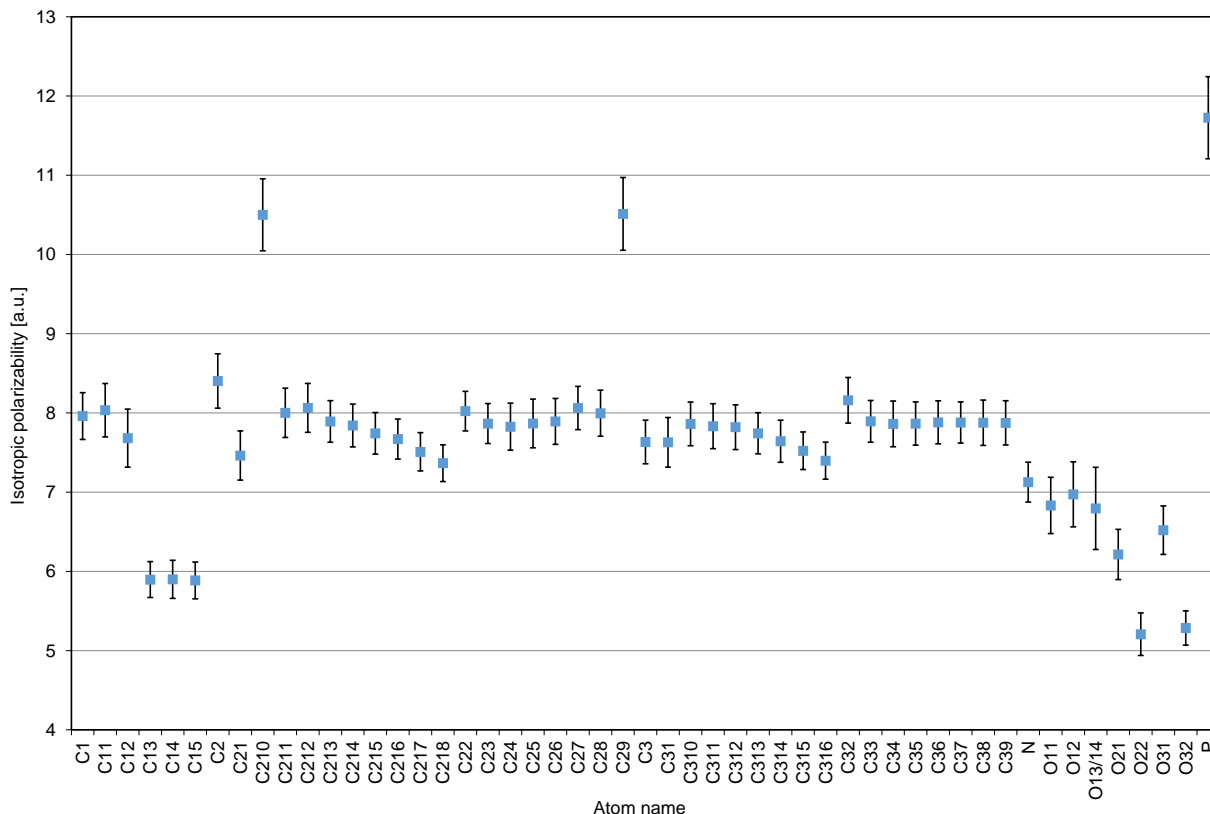


Figure 5: Average (AV) isotropic polarizabilities for atoms in POPC from a simulation in pure water. The AV isotropic polarizabilities for the 200 lipid molecules in the POPC membrane are shown as blue squares, and the standard deviations for the averages as black bars. Only heavy atoms (*i.e.* C, N, O and P) are shown.

Turning to the polarizabilities (illustrated for POPC in Figure 5), we find that polarizabilities for similar atoms cluster together, as also found for solvent molecules.⁶² Thus, all hydrogens have similar values, carbons with only single bonds, oxygens and nitrogen lie within the same range, and the polarizabilities of the double bonded carbons are only exceeded by that of phosphorus. The general tendency for the standard deviations is to increase with increasing average polarizabilities. For the POPS membrane, however, the nitrogen atoms have the largest standard deviation of all the atoms (6.65 ± 0.68), whereas the standard deviation for nitrogen in the PC lipids is only between 0.22 and 0.25 with an average polarizability close to 7. The different behavior for the nitrogen atom in POPS with respect to DMPC and POPC could be due to its close proximity to the negatively charged

carboxylate group in POPS, which is not present in the other lipids. The carboxylate group produces a strong electric field thereby rendering both the charge and polarizability of the nitrogen atom strongly conformation dependent.

To summarize, the isotropic polarizabilities show a small conformational dependence, allowing the average polarizabilities to be used for different conformations.

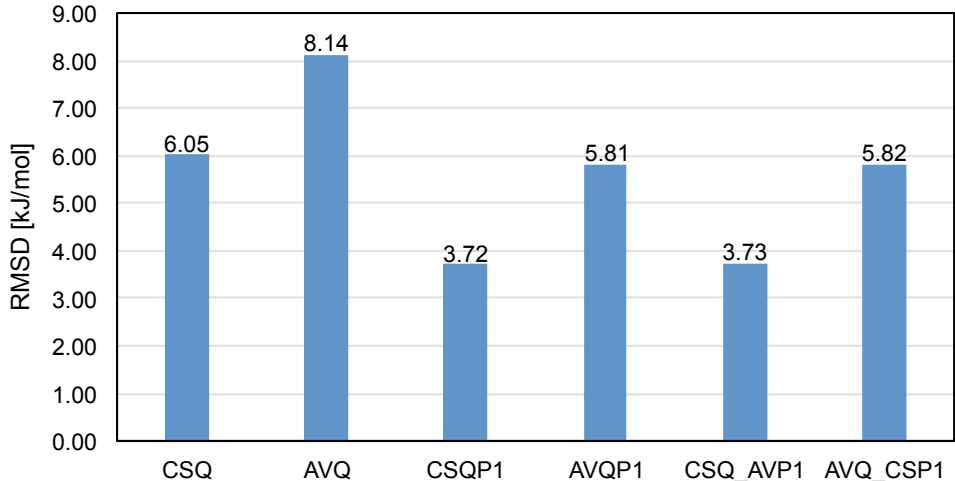


Figure 6: RMSD between the full QM ESP and the ESP calculated with the indicated classical potential (both calculated with B3LYP/aug-cc-pVDZ) of two neighboring DMPC molecules (dilipid). CS = conformation-specific; AV = average; Q = ESP-fitted charge; P1 = isotropic polarizability.

The averaged charges and polarizabilities were tested on the dilipid system to see how well they perform compared to the CS parameters. The ESPs found with CS parameters are compared to the ESPs found with the AV parameters using B3LYP/aug-cc-pVDZ (Figure 6). The RMSD values are larger for the AV parameters than for the CS parameters. Furthermore, Figure 6 shows that if CS charges are combined with AV polarizabilities (CSQ_AVP1), the RMSD values are very close to the ones with pure CS parameters (CSQP1), while if AV charges are combined with CS polarizabilities (AVQ_CSP1), the RMSD values are instead close to those for a pure AV system (AVQP1). It can also be observed that inclusion of polarizabilities reduces the RMSD values by close to 30% both for CS and AV, giving AVQP1 an

RMSD value of 5.54 kJ mol^{-1} , which is within the expected performance of ESPs produced without higher-order multipole moments than charges.⁹⁵

Figure 7 shows the error of ESPs calculated with different force fields as an average over three conformations of DMPC, POPC and POPS. There are some differences between the three lipid conformations in all cases (data not shown), indicating that any force field will not reproduce the QM ESP equally well for all conformations. A clear observation is that the united-atom charges from Chiu *et al.*⁶⁹ reproduce the ESP much poorer than the all-atom force fields. This is not unexpected, since the all-atom force fields are all based on charges fitted to the ESP of several conformations.

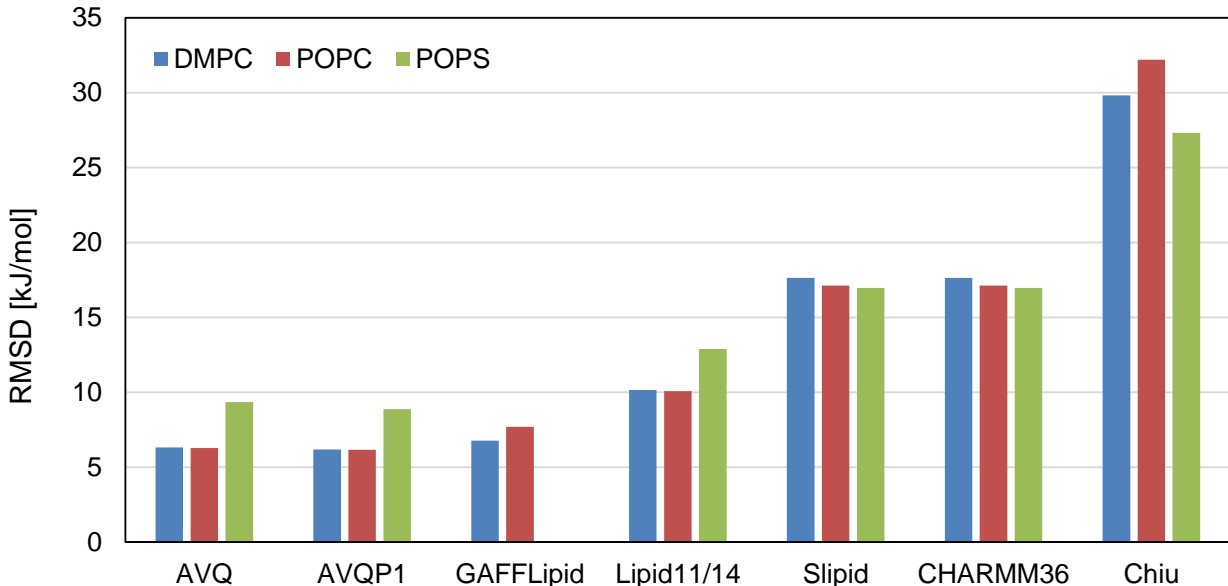


Figure 7: RMSD between the full QM ESP (calculated with B3LYP/aug-cc-pVDZ) and the ESP calculated with the indicated non-polarizable force field for the given lipid type as well as for the average charges (AVQ) and average charges and polarizabilities (AVQP1) developed in this work. The values are averages over three different lipid conformations for each lipid type. Note that GAFFLipid does not have parameters for POPS.

The benefit of the set of parameters developed in this work (*i.e.*, AVQP1) is clearly seen for the dilipid in Figures 3 and 8. While the RMSD values are similar to non-polarizable all-atom force fields for single lipids (Figure 7), they are much lower for the dilipid (Figure 8). Moreover, the average RESP charges obtained in this work (*i.e.*, AVQ) perform better than

any of the previously available all-atom force fields.

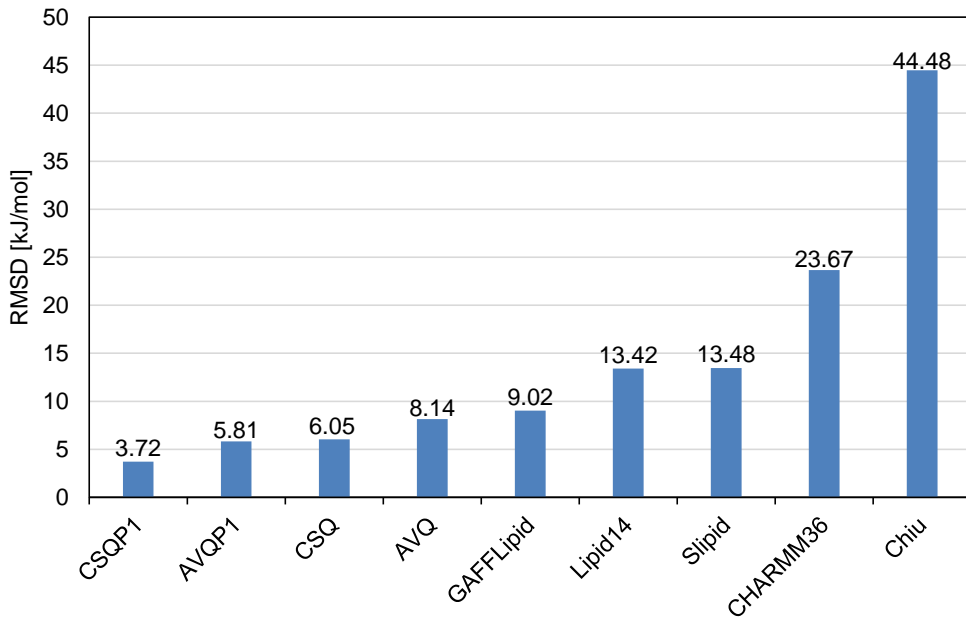


Figure 8: RMSD values between ESPs from full QM calculations and ESPs calculated with either the QP1 parameter sets from this work or charges from standard non-polarizable force fields for the DMPC dilipid system. CS = conformation-specific; AV = average; Q = ESP-fitted charge; P1 = isotropic polarizability.

We expect intermolecular polarization to be even more important for larger lipid systems and conclude that the inclusion of polarizabilities is needed to model the electrostatic component of the MM energy with sufficient accuracy in a full membrane. The inclusion of polarization also allows for a larger flexibility of the electrostatic description when a probe is embedded in the membrane, which is addressed in the following section.

Application: Optical Properties of Prodan

The benefit of using an electrostatic description based on the newly derived parameters over charges from non-polarizable MM force fields is tested in a case study of the probe Prodan in DMPC and POPC lipid membranes. Prodan consists of a naphthalene ring with a dimethylamino substitute on one end and diagonally opposite a propionyl substitute (see the

chemical structure of Prodan in Figure S2 in the supporting information). The amino group and the carbonyl group on either side of the ring system creates a dipole moment along the main axis of Prodan. Upon excitation, the dipole moment increases, and hence a red shift is seen in Prodan’s emission spectrum in polar solvents. The sensitivity of the red shift due to the polarity of the environment renders Prodan a useful membrane probe for the amount of water in the membrane and therefore membrane fluidity.⁹⁶

MD simulations of Prodan were run in either a pure DMPC or a pure POPC membrane (see the supporting information for details), from which a snapshot from each system was extracted. For each membrane system the excitation energy of the lowest singlet transition in Prodan was calculated. For this the electrostatic interaction with the lipid environment was described by increasing accuracy. The lowest level of detail uses only charges for the lipids, the charges being either the AV charges developed in this work (AVQ) or charges from the CHARMM36,⁴⁷ GAFFlipid,⁴³ Lipid14⁴⁵ or Chiu⁶⁹ force fields. The next level includes the AV charges with isotropic polarizabilities, but where the induced dipoles of the lipids are those from the ground state (AVQ-GSP1) that are kept frozen in the linear response calculation of the excited state, *i.e.* including only the static reaction field of the lipids. In the most accurate calculations AV charges and isotropic polarizabilities are again used, but here also the dynamic reaction field of the lipids, as described within a linear response framework, is included (AVQP1).

Table 2 reports the resulting excitation energies, E , together with the magnitude of the ground-state dipole moment, $|\mu|$, and the associated oscillator strength, f , for this transition of Prodan embedded in the DMPC and POPC membranes. Going from vacuum to an increasingly more polarizable environment, *i.e.* from an environment described only by charges (AVQ, CHARMM36, GAFFlipid, Lipid14, Chiu) to one including ground-state polarization (AVQ-GSP1), to including the full polarization within a linear response framework (AVQP1), it is seen for DMPC that the excitation energies become gradually lower, although the trend is not as clear for POPC. Adding charges to the environment lowers the excitation energy by approximately 0.1 eV for DMPC, again the effect is smaller for POPC. Adding ground-state polarization to the AV charges only has little effect on the excitation energies for both POPC and DMPC. However, when the induced dipole moments instead interact with the increased

dipole moment of the excited state, computed to be 12.73 D and 13.48 D for POPC and DMPC, respectively, the excitation energy decreases with around 0.06 eV more than for charges only. By including also the dynamic reaction field we observe a stabilization of the excited state with respect to the ground state. Albeit a numerically small effect, this gradual decrease in excitation energy upon an increasingly polarizable environment underlines the importance of including polarization effects when studying optical properties of a probe like Prodan in different surroundings.

Describing the lipids by the united-atom charges from Chiu *et al.*⁶⁹ has a significantly different effect than the all-atom parameter sets. The united-atom charges result in a smaller dipole moment and larger excitation energy; for DMPC the dipole moment is even smaller and the excitation energy larger than in the vacuum state. Together with ESP surface plots of the difference between the QM ESP and the ESP from Chiu charges in Figure 3h) this clearly shows that united-atom charges are not suitable for use in calculations involving electronic excitations.

	Vacuum					
	$ \mu $	E		f		
VAC	5.69	3.92		0.29		
	POPC			DMPC		
	$ \mu $	E	f	$ \mu $	E	f
AVQ	6.57	3.85	0.32	7.03	3.80	0.30
CHARMM36	6.80	3.83	0.30	7.11	3.81	0.31
GAFFlipid	6.59	3.85	0.32	7.07	3.80	0.31
Lipid14	6.78	3.83	0.32	7.38	3.77	0.31
Chiu	5.53	3.92	0.28	5.78	3.91	0.33
AVQ-GSP1	6.62	3.84	0.32	7.23	3.79	0.32
AVQP1	6.62	3.79	0.45	7.23	3.74	0.44

Table 2: Ground-state dipole moment $|\boldsymbol{\mu}|$ (Debye), excitation energy, E (eV), and oscillator strength, f (dimensionless) for the lowest singlet excited state of Prodan embedded in a POPC or DMPC membrane. Q = RESP charges, P1 = isotropic polarization, GSP1 = polarization described by induced dipole moments in the ground state, *i.e.* the lipid dipole moments are not allowed to change when the electronic configuration of Prodan changes upon excitation. The oscillator strengths calculated with AVQP1 do not include effective external field effects.⁹⁷

CONCLUSIONS

In this paper we have derived a set of average electrostatic parameters for lipid molecules intended to be used in polarizable embedding calculations. Atom-centered charges and polarizabilities are derived for three lipid types commonly employed in both experimental and computational studies, namely DMPC, POPC and POPS. The charges are derived with the RESP method and the isotropic polarizabilities with the LoProp procedure, both at the B3LYP/aug-cc-pVDZ level of theory. Each set of parameters is based on an average over 200 individually calculated charges and polarizabilities obtained from an ensemble of lipid conformations from MD simulations.

A fragmentation strategy was employed to reduce computational cost. Each lipid was fragmented into one head-group fragment and two tail fragments and capping groups were added to mimic the remainder of the lipid. Three different sites of fragmentation were tested together with cap sizes ranging from including the first heavy atom to the first three heavy atoms after the fragmentation site. Differences between the fragmentation schemes were small; the scheme with the lowest error in the ESP compared to full-lipid calculations was chosen for subsequent steps.

The fragmentation procedure was employed on the different membrane structures each consisting of 200 lipid molecules. For a given lipid type significant variations in charges were seen for the same atom in different conformations. The polarizabilities also showed a variation over the different lipid conformations, but significantly less than the charges. Based on the charges and polarizabilities for each lipid in a membrane, average parameters were developed. The average charges naturally reproduce the full QM ESP slightly worse than the charges determined for a specific conformation, but inclusion of polarization alleviates this to some extent. The performance of this average set is much better than that of standard fixed-charge force fields because of the inclusion of polarizabilities. Inclusion of polarization lowered the RMSD values of the ESP compared to the full QM ESP for a system consisting of two neighboring lipid molecules from a membrane. This clearly shows the benefit of including polarizabilities in larger systems, *i.e.* in lipid membranes.

Finally, an example calculation of the membrane probe Prodan embedded in a DMPC or POPC membrane showed the importance of polarization needed for a physically sound description of excitation processes of such probes embedded in membranes.

ACKNOWLEDGMENTS

S.W., M.P. and J.K. acknowledge financial support from the Lundbeck Foundation, the Danish e-Infrastructure Cooperation (DeIC), and the Villum Foundation. N.H.L. acknowledges the Carlsberg Foundation for a postdoctoral fellowship (Grant No. CF15-0792). J.M.H.O. acknowledges financial support from the Danish Council for Independent Research (DFR) through the Sapere Aude research career program (Grant No. DFR-1323-00744 and DFR-1325-00091). J.K. acknowledges financial support from the Danish Council for Indepen-

dent Research (DFF) through the Sapere Aude research career program (Grant No. DFF-0602-02122B). C.S. thanks the Danish Council for Independent Research (the Sapere Aude program) for financial support (Grant No. 4181-00370). M.T.P.B. acknowledges support from the Research Council of Norway through a Centre of Excellence Grant (Grant No. 179568/V30) and from the European Research Council through a Starting Grant (Grant No. 279619). The authors thank Thomas Elmelund Rasmussen for graphical support with the figures.

Additional Supporting Information may be found in the online version of this article.

References

1. Warshel, A. and Levitt, M., *J. Mol. Biol.*, **1976**, 103, 227–249.
2. Senn, H. M. and Thiel, W., *Angew. Chem. Int. Edit.*, **2009**, 48, 1198–1229.
3. Lin, H. and Truhlar, D. G., *Theor. Chem. Acc.*, **2007**, 117, 185–199.
4. Gao, J. and Xia, X., *Science*, **1992**, 258, 631–635.
5. Gao, J.; Habibollahzadeh, D. and Shao, L., *J. Phys. Chem.*, **1995**, 99, 16460–16467.
6. Gao, J.; Pavelites, J. J. and Habibollahzadeh, D., *J. Phys. Chem.*, **1996**, 100, 2689–2697.
7. Xie, W.; Pu, J.; MacKerell Jr., A. D. and Gao, J., *J. Chem. Theory Comput.*, **2007**, 3, 1878–1889.
8. Cieplak, P.; Dupradeau, F.-Y.; Duan, Y. and Wang, J., *J. Phys.: Condens. Mat.*, **2009**, 21, 333102.
9. Söderhjelm, P. and Ryde, U., *J. Phys. Chem. A*, **2009**, 113, 617–627.
10. Vorobyov, I. V.; Anisimov, V. M. and MacKerell Jr., A. D., *J. Phys. Chem. B*, **2005**, 109, 18988–18999.
11. Allen, T. W.; Andersen, O. S. and Roux, B., *Proc. Natl. Acad. Sci. USA*, **2003**, 101, 117–122.

12. Allen, T. W.; Andersen, O. S. and Roux, B., *Biophys. J.*, **2006**, 90, 3447–3468.
13. Lopes, P. E. M.; Roux, B. and MacKerell Jr., A. D., *Theor. Chem. Acc.*, **2009**, 124, 11–28.
14. Applequist, J.; Carl, J. R. and Fung, K.-K., *J. Am. Chem. Soc.*, **1972**, 94, 2952–2960.
15. Ren, P. and Ponder, J. W., *J. Comput. Chem.*, **2002**, 23, 1497–1506.
16. Ren, P. and Ponder, J. W., *J. Phys. Chem. B*, **2003**, 107, 5933–5947.
17. Cieplak, P.; Caldwell, J. and Kollman, P., *J. Comput. Chem.*, **2001**, 22, 1048–1057.
18. Kaminski, G. A.; Ponomarev, S. Y. and Liu, A. B., *J. Chem. Theory Comput.*, **2009**, 5, 2935–2943.
19. Lamoureux, G. and Roux, B., *J. Chem. Phys.*, **2003**, 119, 3025–3039.
20. Lamoureux, G.; MacKerell Jr., A. D. and Roux, B., *J. Chem. Phys.*, **2003**, 119, 5185–5197.
21. Harder, E.; MacKerell Jr., A. D. and Roux, B., *J. Am. Chem. Soc.*, **2009**, 131, 2760–2761.
22. Vorobyov, I. and Allen, T. W., *J. Chem. Phys.*, **2010**, 132, 185101.
23. Chowdhary, J.; Harder, E.; Lopes, P. E. M.; Huang, L.; MacKerell Jr., A. D. and Roux, B., *J. Phys. Chem. B*, **2013**, 117, 9142–9160.
24. Robinson, D., *J. Chem. Theory Comput.*, **2013**, 9, 2498–2503.
25. Cornell, W. D.; Cieplak, P.; Bayly, C. I.; Gould, I. R.; Merz, K. M.; Ferguson, D. M.; Spellmeyer, D. C.; Fox, T.; Caldwell, J. W. and Kollman, P. A., *J. Am. Chem. Soc.*, **1995**, 117, 5179–5197.
26. Hornak, V.; Abel, R.; Okur, A.; Strockbine, B.; Roitberg, A. and Simmerling, C., *Proteins*, **2006**, 65, 712–725.

27. Bayly, C. I.; Cieplak, P.; Cornell, W. and Kollman, P. A., *J. Phys. Chem.*, **1993**, 97, 10269–10280.
28. Besler, B. H.; Merz, K. M. and Kollman, P. A., *J. Comput. Chem.*, **1990**, 11, 431–439.
29. Hu, H.; Lu, Z. and Yang, W., *J. Chem. Theory Comput.*, **2007**, 3, 1004–1013.
30. Breneman, C. M. and Wiberg, K. B., *J. Comput. Chem.*, **1990**, 11, 361–373.
31. Williams, D. E., *Biopolymers*, **1990**, 29, 1367–1386.
32. Stouch, T. and Williams, D. E., *J. Comput. Chem.*, **1992**, 13, 622–632.
33. Reynolds, C. A.; Essex, J. W. and Richards, W. G., *Chem. Phys. Lett.*, **1992**, 199, 257–260.
34. Pacios, L. and Gómez, P., *J. Mol. Struc.*, **2001**, 544, 237–251.
35. Söderhjelm, P. and Ryde, U., *J. Comput. Chem.*, **2009**, 30, 750–760.
36. Stouch, T. R. and Williams, D. E., *J. Comput. Chem.*, **1993**, 14, 858–866.
37. Söderhjelm, P.; Kongsted, J. and Ryde, U., *J. Chem. Theory Comput.*, **2011**, 7, 1404–1414.
38. Olsen, J. M.; Aidas, K. and Kongsted, J., *J. Chem. Theory Comput.*, **2010**, 6, 3721–3734.
39. Olsen, J. M. H. and Kongsted, J., *Adv. Quantum Chem.*, **2011**, 61, 107–143.
40. Jämbeck, J. P. M. and Lyubartsev, A. P., *J. Phys. Chem. B*, **2012**, 116, 3164–3179.
41. Jämbeck, J. P. M. and Lyubartsev, A. P., *J. Chem. Theory Comput.*, **2012**, 8, 2938–2948.
42. Jämbeck, J. P. M. and Lyubartsev, A. P., *J. Chem. Theory Comput.*, **2013**, 9, 774–784.
43. Dickson, C. J.; Rosso, L.; Betz, R. M.; Walker, R. C. and Gould, I. R., *Soft Matter*, **2012**, 8, 9617–9627.

44. Skjevik, Å.; Madej, B. D.; Walker, R. C. and Teigen, K., *J. Phys. Chem. B*, **2012**, 116, 11124–11136.
45. Dickson, C. J.; Madej, B. D.; Skjevik, Å.; Betz, R. M.; Teigen, K.; Gould, I. R. and Walker, R. C., *J. Chem. Theory Comput.*, **2014**, 10, 865–879.
46. Case, D.; Darden, T.; Cheatham III, T.; Simmerling, C.; Wang, J.; Duke, R.; Luo, R.; Walker, R.; Zhang, W.; Merz, K.; Roberts, B.; Hayik, S.; Roitberg, A.; Seabra, G.; Swails, J.; Götz, A.; Kolossváry, I. Wong, K.; Paesani, F.; Vanicek, J.; Wolf, R.; Liu, J.; Wu, X.; Brozell, S.; Steinbrecher, T.; Gohlke, H.; Cai, Q.; Ye, X.; Wang, J.; Hsieh, M.-J.; Cui, G.; Roe, D.; Mathews, D.; Seetin, M.; Salomon-Ferrer, R.; Sagui, C.; Babin, V.; Luchko, T.; Gusarov, S.; Kovalenko, A. and Kollman, P., *Amber 12*, 2012.
47. Klauda, J. B.; Venable, R. M.; Freites, J. A.; O’Connor, J. W.; Tobias, D. J.; Mondragon-Ramirez, C.; Vorobyov, I.; MacKerell Jr., A. D. and Pastor, R. W., *J. Phys. Chem. B*, **2010**, 114, 7830–7843.
48. Jorgensen, W. L.; Chandrasekhar, J.; Madura, J. D.; Impey, R. W. and Klein, M. L., *J. Chem. Phys.*, **1983**, 79, 926–935.
49. Zhang, D. W. and Zhang, J. Z. H., *J. Chem. Phys.*, **2003**, 119, 3599–3605.
50. Steinmann, C.; Ibsen, M. W.; Hansen, A. S. and Jensen, J. H., *PLOS ONE*, **2012**, 7, e44480.
51. Frisch, M. J.; Trucks, G. W.; Schlegel, H. B.; Scuseria, G. E.; Robb, M. A.; Cheeseman, J. R.; Scalmani, G.; Barone, V.; Mennucci, B.; Petersson, G. A.; Nakatsuji, H.; Caricato, M.; Li, X.; Hratchian, H. P.; Izmaylov, A. F.; Bloino, J.; Zheng, G.; Sonnenberg, J. L.; Hada, M.; Ehara, M.; Toyota, K.; Fukuda, R.; Hasegawa, J.; Ishida, M.; Nakajima, T.; Honda, Y.; Kitao, O.; Nakai, H.; Vreven, T.; Montgomery, Jr., J. A.; Peralta, J. E.; Ogliaro, F.; Bearpark, M.; Heyd, J. J.; Brothers, E.; Kudin, K. N.; Staroverov, V. N.; Kobayashi, R.; Normand, J.; Raghavachari, K.; Rendell, A.; Burant, J. C.; Iyengar, S. S.; Tomasi, J.; Cossi, M.; Rega, N.; Millam, J. M.; Klene, M.; Knox, J. E.; Cross, J. B.; Bakken, V.; Adamo, C.; Jaramillo, J.; Gomperts, R.; Stratmann, R. E.; Yazyev, O.;

- Austin, A. J.; Cammi, R.; Pomelli, C.; Ochterski, J. W.; Martin, R. L.; Morokuma, K.; Zakrzewski, V. G.; Voth, G. A.; Salvador, P.; Dannenberg, J. J.; Dapprich, S.; Daniels, A. D.; Farkas, O.; Foresman, J. B.; Ortiz, J. V.; Cioslowski, J. and Fox, D. J., Gaussian 09 Revision D.0.
52. Wang, J.; Wang, W.; Kollman, P. A. and Case, D. A., *J. Mol. Graph. Model.*, **2006**, 25, 247–260.
 53. Wang, B. and Merz, K. M., *J. Chem. Theory Comput.*, **2006**, 2, 209–215.
 54. Sigfridsson, E. and Ryde, U., *J. Comput. Chem.*, **1998**, 19, 377–395.
 55. Gagliardi, L.; Lindh, R. and Karlström, G., *J. Chem. Phys.*, **2004**, 121, 4494–4500.
 56. Karlström, G.; Lindh, R.; Malmqvist, P.-Å.; Roos, B. O.; Ryde, U.; Veryazov, V.; Widmark, P.-O.; Cossi, M.; Schimmelpfennig, B.; Neogrady, P. and Seijo, L., *Comp. Mater. Sci.*, **2003**, 28, 222–239.
 57. Aquilante, F.; De Vico, L.; Ferré, N.; Ghigo, G.; Malmqvist, P.-Å.; Neogrady, P.; Pedersen, T. B.; Pitoňák, M.; Reiher, M.; Roos, B. O.; Serrano-Andrés, L.; Urban, M.; Veryazov, V. and Lindh, R., *J. Comput. Chem.*, **2010**, 31, 224–247.
 58. Olsen, J. M. H.; List, N. H.; Kristensen, K. and Kongsted, J., *J. Chem. Theory Comput.*, **2015**, 11, 1832–1842.
 59. Dunning, T. H., *J. Chem. Phys.*, **1989**, 90, 1007–1023.
 60. Kendall, R. A.; Dunning, T. H. and Harrison, R. J., *J. Chem. Phys.*, **1992**, 96, 6796–6806.
 61. Woon, D. E. and Dunning, T. H., *J. Chem. Phys.*, **1993**, 98, 1358–1371.
 62. Beerepoot, M. T. P.; Steindal, A. H.; List, N. H.; Kongsted, J. and Olsen, J. M. H., *J. Chem. Theory Comput.*, **2016**.
 63. Becke, A. D., *J. Chem. Phys.*, **1993**, 98, 5648–5652.

64. Lee, C.; Yang, W. and Parr, R. G., *Phys. Rev. B*, **1988**, 37, 785–789.
65. Vosko, S. H.; Wilk, L. and Nusair, M., *Can. J. Phys.*, **1980**, 58, 1200–1211.
66. Stephens, P. J.; Devlin, F. J.; Chabalowski, C. F. and Frisch, M. J., *J. Phys. Chem.*, **1994**, 98, 11623–11627.
67. Becke, A. D., *Phys. Rev. A*, **1988**, 38, 3098–3100.
68. Schwabe, T.; Olsen, J. M. H.; Sneskov, K.; Kongsted, J. and Christiansen, O., *J. Chem. Theory Comput.*, **2011**, 7, 2209–2217.
69. Chiu, S.-W.; Clark, M.; Balaji, V.; Subramaniam, S.; Scott, H. L. and Jakobsson, E., *Biophys. J.*, **1995**, 69, 1230–1245.
70. Poger, D. and Mark, A. E., *J. Chem. Theory Comput.*, **2010**, 6, 325–336.
71. Kukol, A., *J. Chem. Theory Comput.*, **2009**, 5, 615–626.
72. Chiu, S.-W.; Pandit, S. A.; Scott, H. L. and Jakobsson, E., *J. Phys. Chem. B*, **2009**, 113, 2748–2763.
73. Berger, O.; Edholm, O. and Jähnig, F., *Biophys. J.*, **1997**, 72, 2002–2013.
74. Domański, J.; Stansfeld, P. J.; Sansom, M. S. P. and Beckstein, O., *J. Membrane Biol.*, **2010**, 236, 255–258.
75. Case, D. A.; Babin, V.; Berryman, J. T.; Betz, R. M.; Cai, Q.; Cerutti, D. S.; Cheatham III, T. E.; Darden, T. A.; Duke, R. E.; Gohlke, H.; Götz, A.; Gusarov, S.; Homeyer, N.; Janowski, P.; Kaus, J.; Kolossváry, I.; Kovalenko, A.; Lee, T. S.; LeGrand, S.; Luchko, T.; Luo, R.; Madej, B.; Merz, K. M.; Paesani, F.; Roe, D. R.; Roitberg, A.; Sagui, C.; Salomon-Ferrer, R.; Seabra, G.; Simmerling, C. L.; Smith, W.; Swails, J.; Walker, R. C.; Wang, J.; Wolf, R. M.; Wu, X. and Kollman, P. A., *Amber 14*, 2014.
76. Wu, E. L.; Cheng, X.; Jo, S.; Rui, H.; Song, K. C.; Dávila-Contreras, E. M.; Qi, Y.; Lee, J.; Monje-Galvan, V.; Venable, R. M.; Klauda, J. B. and Im, W., *J. Comput. Chem.*, **2014**, 35, 1997–2004.

77. Olsen, J. M. H., PELib: The Polarizable Embedding library (version 1.0.8), 2014.
78. Aidas, K.; Angeli, C.; Bak, K. L.; Bakken, V.; Bast, R.; Boman, L.; Christiansen, O.; Cimiraglia, R.; Coriani, S.; Dahle, P.; Dalskov, E. K.; Ekström, U.; Enevoldsen, T.; Eriksen, J. J.; Ettenhuber, P.; Fernández, B.; Ferrighi, L.; Fliegl, H.; Frediani, L.; Hald, K.; Halkier, A.; Hättig, C.; Heiberg, H.; Helgaker, T.; Hennum, A. C.; Hetttema, H.; Hjertenæs, E.; Høst, S.; Høyvik, I.-M.; Iozzi, M. F.; Jansik, B.; Jensen, H. J. Aa.; Jonsson, D.; Jørgensen, P.; Kauczor, J.; Kirpekar, S.; Kjærgaard, T.; Klopper, W.; Knecht, S.; Kobayashi, R.; Koch, H.; Kongsted, J.; Krapp, A.; Kristensen, K.; Ligabue, A.; Lutnæs, O. B.; Melo, J. I.; Mikkelsen, K. V.; Myhre, R. H.; Neiss, C.; Nielsen, C. B.; Norman, P.; Olsen, J.; Olsen, J. M. H.; Osted, A.; Packer, M. J.; Pawłowski, F.; Pedersen, T. B.; Provati, P. F.; Reine, S.; Rinkevicius, Z.; Ruden, T. A.; Ruud, K.; Rybkin, V.; Salek, P.; Samson, C. C. M.; Sánchez de Merás, A.; Saue, T.; Sauer, S. P. A.; Schimmelpfennig, B.; Sneskov, K.; Steindal, A. H.; Sylvester-Hvid, K. O.; Taylor, P. R.; Teale, A. M.; Tellgren, E. I.; Tew, D. P.; Thorvaldsen, A. J.; Thøgersen, L.; Vahtras, O.; Watson, M. A.; Wilson, D. J. D.; Ziolkowski, M. and Ågren, H., *WIREs Comput. Mol. Sci.*, **2013**, 4, 269–284.
79. LSDalton, a linear scaling molecular electronic structure program, Release LSDalton2013 (2013), see <http://daltonprogram.org/>.
80. Jensen, F., *J. Chem. Theory Comput.*, **2010**, 6, 2726–2735.
81. Jakobsen, S.; Kristensen, K. and Jensen, F., *J. Chem. Theory Comput.*, **2013**, 9, 3978–3985.
82. Krishnan, R.; Binkley, J. S.; Seeger, R. and Pople, J. A., *J. Chem. Phys.*, **1980**, 72, 650–654.
83. McLean, A. D. and Chandler, G. S., *J. Chem. Phys.*, **1980**, 72, 5639–5648.
84. Clark, T.; Chandrasekhar, J.; Spitznagel, G. W. and Von Ragué Schleyer, P., *J. Comput. Chem.*, **1983**, 4, 294–301.
85. Frisch, M. J.; Pople, J. A. and Binkley, J. S., *J. Chem. Phys.*, **1984**, 80, 3265–3269.

86. Tomasi, J.; Mennucci, B. and Cancès, E., *J. Mol. Struct. THEOCHEM*, **1999**, 464, 211–226.
87. Scalmani, G. and Frisch, M. J., *J. Chem. Phys.*, **2010**, 132, 114110.
88. Dalton, A Molecular Electronic Structure Program, Release DALTON2013.2 (2013), see <http://daltonprogram.org/>.
89. Gao, B., Gen1Int Version 0.2.1, 2012.
90. Gao, B.; Thorvaldsen, A. J. and Ruud, K., *Int. J. Quantum Chem.*, **2011**, 111, 858–872.
91. Yanai, T.; Tew, D. P. and Handy, N. C., *Chem. Phys. Lett.*, **2004**, 393, 51–57.
92. Hehre, W. J.; Ditchfield, R. and Pople, J. A., *J. Chem. Phys.*, **1972**, 56, 2257–2261.
93. Hariharan, P. C. and Pople, J. A., *Theor. Chim. Acta*, **1973**, 28, 213–222.
94. Francel, M. M.; Pietro, W. J.; Hehre, W. J.; Binkley, J. S.; Gordon, M. S.; DeFrees, D. J. and Pople, J. A., *J. Chem. Phys.*, **1982**, 77, 3654–3665.
95. Jakobsen, S. and Jensen, F., *J. Chem. Theory Comput.*, **2014**, 10, 5493–5504.
96. Parasassi, T.; Krasnowska, E. K.; Bagatolli, L. and Gratton, E., *J. Fluoresc.*, **1998**, 8, 365–373.
97. List, N. H.; Jensen, H. J. A. and Kongsted, J., *Phys. Chem. Chem. Phys.*, **2016**, 18, 10070–10080.